Grain refinement in a commercial Al–Mg–Sc alloy under hot ECAP conditions

O. Sitdikov [a,b,*], T. Sakai [c], E. Avtokratova [b], R. Kaibyshev [b], Y. Kimura [a], K. Tsuzaki [a]

[a] *National Institute for Materials Science, Tsukuba 305-0047, Japan*
[b] *Institute for Metals Superplasticity Problems, Khalturina 39, Ufa 450001, Russia*
[c] *Department of Mechanical Engineering and Intelligent Systems, UEC Tokyo (University of Electro-Communications), Chofu, Tokyo 182-8585, Japan*

Abstract

Grain refinement taking place during equal-channel angular pressing (ECAP) was studied in a commercial Al–6% Mg–0.4% Mn–0.3% Sc alloy at a temperature of 450 °C ($\sim 0.8T_m$) to demonstrate the feasibility of obtaining new fine-grained structure in a hard-to-deform Al–Mg–Sc alloy under hot intense plastic straining (IPS) conditions and investigate the evolution process of new grains. Inhomogeneous deformation occurring during hot ECAP leads to formation of deformation bands. Repeated ECAP results in mutual crossing and increase in number and the misorientation of deformation bands, followed by transformation of the boundaries of deformation bands into high-angle ones. As a result, a new fine-grained microstructure with an average crystallite size of 2.8 μm develops at large strains above 8. It is concluded that grain refinement occurs in accordance with deformation-induced continuous reactions; that is similar to in-situ or continuous dynamic recrystallization. The mechanisms of new grain evolution, as well as factors promoting grain refinement, are discussed in detail.

Keywords: Intense plastic straining (IPS); Aluminum alloys; Hot working; Equal-channel angular pressing (ECAP); Grain refining; Deformation bands

1. Introduction

Grain refinement of commercial-base Al alloys to a submicron scale level is one of the major interests in a case, when an ultrahigh strength–ductility combination is required for practical application or when superplastic forming is involved for the manufacturing of various parts or details [1]. Equal-channel angular pressing (ECAP) is a relatively new metalworking process, which is capable of producing such fine-grained structures by means of intense plastic straining (IPS), i.e. when ultrahigh strains can be imposed on the worked material without a change in their shape or dimensions [1–42]. Cold-to-warm working by the ECAP has been shown to result in the formation of submicrocrystalline structures in numerous Al alloys [3,5–10,14–20,22–29,31–34,36,37,39]. The new ultrafine grains could be evolved in accordance with a mechanism of continuous dynamic recrystallization (cDRX) [43,44]. Namely, some low-to-medium angle subboundaries, sometimes called as *deformation bands* or *geometrically necessary boundaries* [45], may be generated within the original grains at relatively low strains due to strain heterogeneity and result in grain subdivision [11,13,14,17,28,29,36,37]. They are progressively transformed into high-angle boundaries with further deformation leading to full development of new grain structures in large strain.

Some heavily alloyed Al alloys are categorized, however, as hard plastic materials, which are sometimes hardly deformed by ECAP because of a limited ductility and formability at low-to-intermediate temperatures. First, intense shearing occurring during each pass in ECAP can result frequently in a premature failure of such materials that makes impossible to apply IPS (e.g. [18,20,40]). Second, it may be difficult to completely fill the die corner at the point where the two channels intersect [4]. At last, high pressure is required to successfully press the sample through the die and problems may arise because of a breaking of the die or the plunger. Increasing pressing temperature, in contrast, could normally lead to improvement in the plastic workability. This can also provide a great benefit from decreasing strength of material, which makes ECAP much easier. With these advantages, ECAP performed at elevated temperatures

* Corresponding author. Present address: Nagoya Institute of Technology, Nagoya 466-8555, Japan. Tel./fax: +81 527 35 5293.
E-mail address: sitdikov.oleg@nitech.ac.jp (O. Sitdikov).

could be very promising technical approach having a great commercial potential. Unfortunately, little is known presently about the effect of processing temperature on microstructural development during ECAP. While some experimental evidence of new fine grain formation during warm-to-hot ECAP has been presented and discussed for Al alloys in the recent publications [8,11–13,19,21,30,31,38,40], factors affecting grain refinement and the *mechanisms* of deformation-induced grain formation are currently a matter of some debates and not clear due to an insufficiency of the related experimental data.

The aim of the present research was to study the microstructural evolution in a commercial coarse-grained Al–6% Mg–0.3% Sc alloy subjected to ECAP at $T = 450\,^{\circ}C$ (about $0.8T_m$). This alloy belongs to a class of advanced structural materials, exhibiting ultrahigh strength at ambient temperature [46]. It can be easily hot worked, while cold forming causes many problems because of high yield stress and relatively low ductility. Accordingly, an evaluation of potentiality of the grain scaling in large scale billets seems to be very important for commercial application. In the current work, the starting material was a pre-extruded rod with elongated grains having a stable (sub)grain structure with low-to-moderate angle misorientation resulted from previous working and annealing operations. These crystallites were expected to play a significant role in the initiation of new grain formation during subsequent hot deformation [43]. Specific attention was paid to elucidate main factors promoting grain refinement in this alloy under hot ECAP conditions and to discuss the mechanism of grain formation.

2. Experimental

The alloy used had the following chemical composition (in mass%): 6Mg, 0.4Mn, 0.3Sc, 0.2Si, 0.1Fe and the balance Al. It was fabricated by casting into a steel mold at the Kamensk-Uralsk Metallurgical Works (Russia), and then homogenized at 520 °C for 48 h. Extrusion was performed at 390 °C to a strain of about 0.7, followed by annealing at 400 °C for 1 h. The alloy had a non-uniform microstructure with a bimodal distribution of the grain size, namely coarse elongated grains lying parallel to the extrusion axis, and fine equiaxed grains in their grain boundary regions. The size of coarse grains varied from 150 to 200 μm and from 50 to 100 μm in longitudinal and transverse directions, respectively. The fine grains had the average size of 4.4 μm with a volume fraction of about 0.35. Two different types of dispersion particles were identified by TEM as coherent Al_3Sc dispersoids having a size from 10 to 20 nm, and incoherent Al_6Mn precipitates having a size of about 200 nm [17].

Samples for ECAP were machined parallel to the extrusion axis into rods with a diameter of 20 mm and a length of around 100 mm. ECAP was carried out at 450 °C using a circular die in cross-section with a diameter of 20 mm. The die had a channel in L-shaped configuration with an angle of 90° between the two channels and an angle 0° at the outer arc curvature at the point of intersection. These angles lead to a strain of about 1 in each passage through the die. A heating jacket was put on the die and the pressing temperature was controlled within ±5 °C of 450 °C. Samples were pressed repeatedly up to a strain of 12 using route A, i.e. the orientation of billet was not changed at each pass. The route A was selected in the present work because the recent experiments on Al alloys have shown that it is the most efficient processing route for forming a fine grain structure with larger fraction of high-angle boundaries (HABs) [9,30]. Second, this is *the simplest method* of ECAP and hence it can be most suitable for grain refinement under industrial conditions. The ECAP was performed in a hydraulic press operating at a pressing speed of ~6 mm/s. In accordance with [47] this provided the average effective strain rate, $\dot{\varepsilon}_{eff} \sim 3\,s^{-1}$. The samples pressed were quenched in water after each deformation pass and then reheated at 450 °C during 45 min before next ECAP.

Samples for hardness measurement, optical microscopy, electron back scattering diffraction pattern (EBSP) and transmission electron microscopy (TEM) analyses were cut from central places of the pressed rods in longitudinal section parallel to the pressing direction. Vickers hardness of the samples pressed was measured at room temperature with a load of 1 N. Samples for optical microscopy were annealed at 170 °C for 4 h in order to decorate HABs by secondary phase particles [35]. These grain-boundary precipitates were then revealed by etching with a standard Keller's reagent. The metallographic observations were carried out using a Neophot-32 optical microscope. The volume fraction of fine grains was derived from optical microscopy using an Epiquant structure analyzer operating in semi-automatic regime. (Sub)grain boundary misorientation distributions were obtained from EBSP by using LEO1530 scanning electron microscope (SEM). The examining areas were automatically scanned in 0.3 μm step. Over the misorientation parameters measured by EBSP, the boundaries with misorientation less than 2° were not taken into account. Specimens for TEM examination were mechanically ground to a thickness of about 200 μm and electro-polished in a solution of 30% HNO_3 and 70% CH_3OH at a temperature of −30 °C using a Tenupol-3 twin-jet polishing unit at 20 V. They were then examined using a JEOL-2000EX TEM. The mean crystallite size was measured by: (i) optical microscopy allowing determination of the size of fine grains surrounded by HABs; (ii) TEM for (sub)grains surrounded by both HABs and low-angle boundaries (LABs); and (iii) EBSP for crystallites with misorientation from 10°, i.e. that surrounded by moderate and high-angle boundaries. In (i) and (ii), the line-intercept method was implemented for measurements. In (iii), individual grains were automatically identified with EBSP and defined as areas being completely bounded by boundaries having a misorientation angle equal or larger than a critical value of 10°. The grain size parameter was calculated as an average length of minor and major axes of ellipse fitted on a grain.

3. Results

3.1. Room temperature hardness

Vickers hardness measured at room temperature is plotted against the number of pressings in Fig. 1. The hardness change during static annealing at 450 °C is also represented in Fig. 1

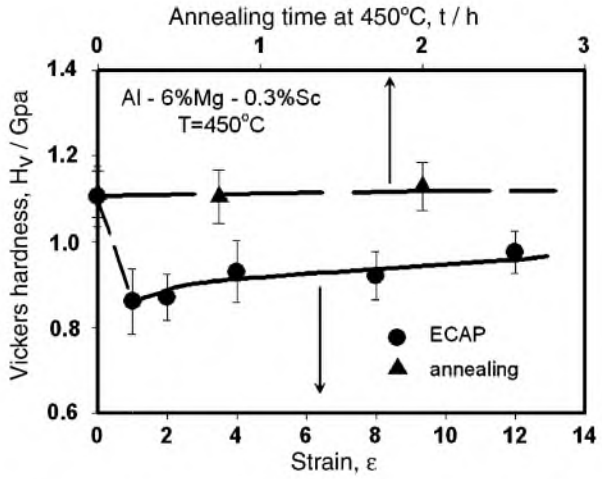

Fig. 1. Hardness changes in Al–6% Mg–0.3% Sc alloy after ECAP and static annealing at 450 °C.

for comparison. It is seen that the hardness of the original material is not remarkably changed during annealing. These data are in agreement with the results of Ref. [20], indicating that heavily warm worked Al-Mg–Sc alloys do not exhibit drastic decrease in the hardness during annealing up to 500 °C, since the deformation microstructure remains stable due to Sc additions. This suggests that any static restoration processes (namely static recrystallization and recovery) can hardly occur during reheating of the present alloy just before hot ECAP; that is any structural changes in the deformed samples can be mainly affected by accumulation of strains applied in each ECAP pass. It is seen in Fig. 1, in contrast, that the hardness drops rapidly from around 1.1 GPa in the initial state to around 0.85 GPa just after the first pass through the ECAP die and, subsequently, starts to increase with increasing the number of pressings. Such decrease of hardness after a first pressing is because of the work softening that is caused mostly by a rearrangement of dislocation/subgrain structures during hot ECAP, as it will be discussed later. At moderate-to-high strains of over 3, the hardness of material grows very slowly at almost constant strain hardening rate, achieving a value of about 0.95 GPa at $\varepsilon = 12$. Such hardening behavior of the microstructure produced by hot ECAP, at which there is no difference in the strain hardening with increasing the number of pressings can be comparable with that of some Al alloys ECAPed at low and intermediate temperatures [12,39]. This may be attributed to dynamic recovery controlling the structural changes during such repetitive hot deformation [12,43].

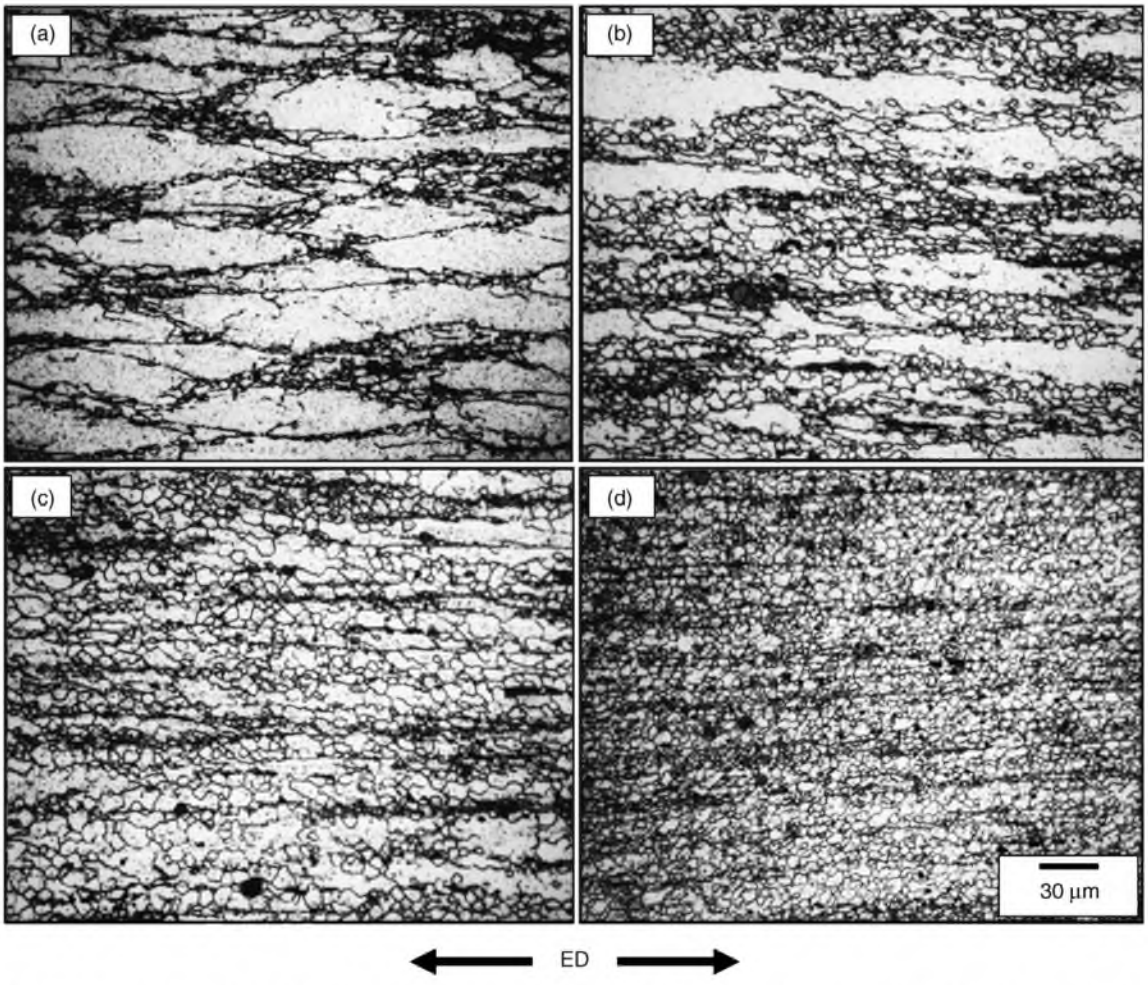

Fig. 2. Typical microstructures developed in Al–6% Mg–0.3% Sc alloy during ECAP at 450 °C: (a) $\varepsilon = 0$, (b) $\varepsilon = 1$, (c) $\varepsilon = 4$ and (d) $\varepsilon = 12$. ED is the extrusion direction.

3.2. Deformation microstructure

A series of typical microstructures (a) before ECAP ($\varepsilon = 0$) and (b)–(d) evolved during ECAP to $\varepsilon = 1$–12 is represented in Fig. 2. It is seen that original elongated grains presented in initial structure (Fig. 2(a)) are pancaked along the extrusion direction (ED) and, concurrently, new fine grains are created along such coarse grain boundaries. At $\varepsilon = 1$, new grains are frequently evolved in coarse grain interiors as necklace-like rings (Fig. 2(b)). With further ECAP, they progressively propagate from mantle regions to grain interiors and, at higher strains, the regions of fine grains and remnant original grains become distributed more homogeneously (Fig. 2(c)). At a strain of 12, the initial coarse-grained microstructure is almost fully replaced by new fine-grained one (Fig. 2(d)).

3.3. OIM microstructures

Fig. 3 shows typical structures observed by orientation imaging microscopy (OIM) at (a) $\varepsilon = 0$, (b) $\varepsilon = 1$ and (c) $\varepsilon = 2$. Here the different grayscale levels indicate the different crystallographic orientation and the differences between neighboring grid points $2^\circ < \Theta < 15^\circ$ and $\Theta > 15^\circ$ are marked by narrow and bold black lines, respectively. It is seen in Fig. 3(a) that the alloy just

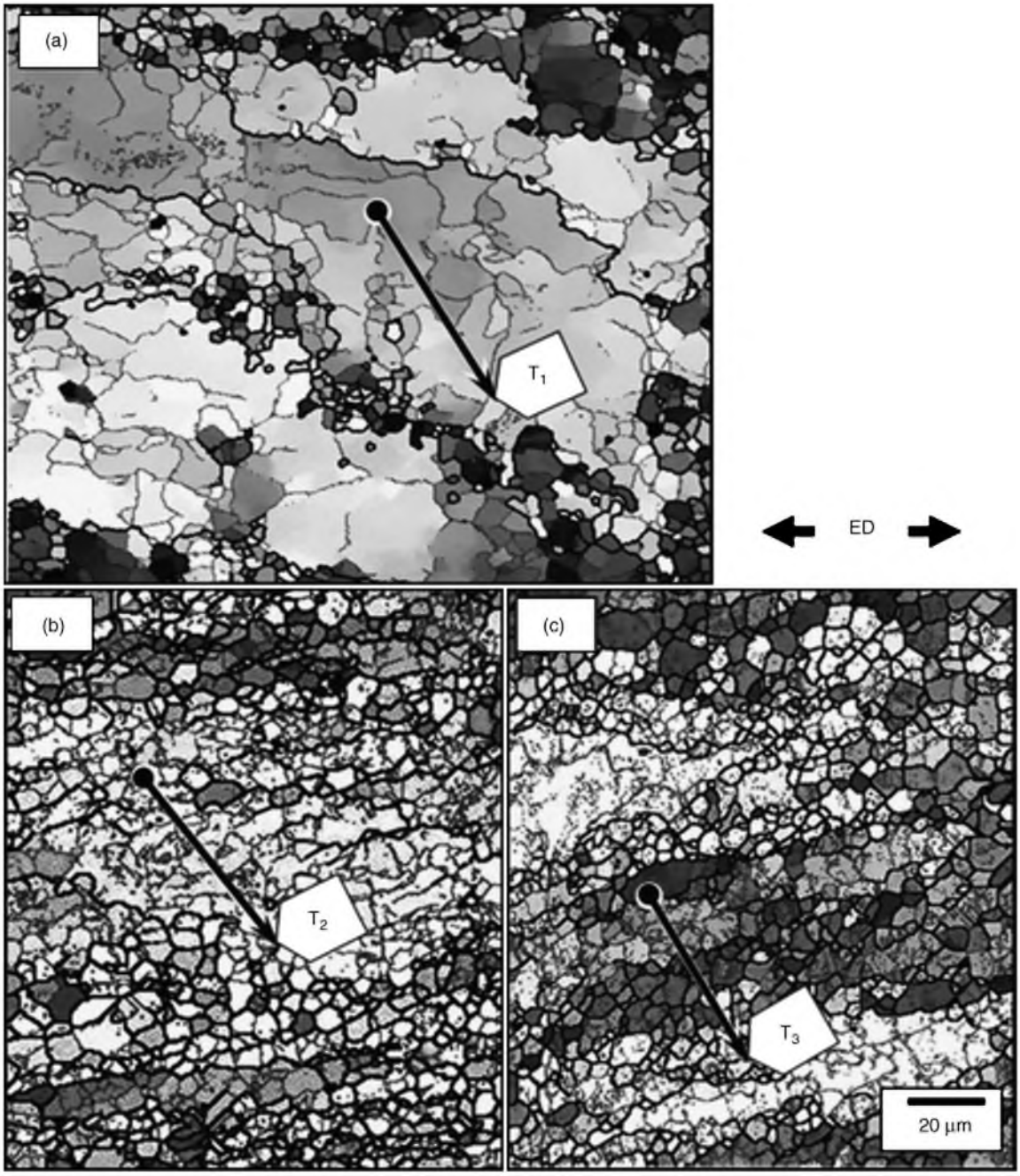

Fig. 3. Typical OIM maps of the microstructure evolved during ECAP at: (a) $\varepsilon = 0$, (b) $\varepsilon = 1$ and (c) $\varepsilon = 2$. ED is the extrusion direction.

before ECAP contained a high density of dislocation subboundaries with low-to-moderate misorientation angles. Their average misorientation angle was around 5°. The mean crystallite size fragmented by these boundaries was in the range of 3–30 μm. During hot ECAP, new fine grains surrounded by HABs (bold lines) and dislocation subboundaries with low-to-medium angle misorientations (narrow lines) are frequently evolved along the original grain boundaries and in grain interiors, respectively. After the first pass through the die, several sets of subboundaries can be observed within initial coarse grains (Fig. 3(b)). They are developed in various directions and fragment the original grains into small separate misoriented domains. Some of them are transformed into new fine grains, frequently in the grain boundary regions and occasionally in the original grain interiors. At a strain of 2, the deformation microstructure comprises banded arrays of intergranular boundaries with a large fraction of HABs (Fig. 3(c)). The new fine grains with high misorientation boundaries are frequently but inhomogeneously developed in the grain boundary regions and within the banded areas accompanying with evolution of the relatively coarse crystallites surrounded by both HABs and LABs. The fraction of HABs is gradually increased by the following ECAP to strains beyond 4 and so, with further evolution of such fine grain structures proceeding more homogeneously in the whole area.

Fig. 4(a–c) represents the distribution of typical point-to-point ($\Delta\Theta$) misorientations developed along the lines T_1, T_2 and T_3 indicated in Fig. 3. The value of $\Delta\Theta$ defines the relative difference in crystal orientation between two neighboring scan points with step of 0.3 μm. The line length T was selected to be commensurate with the original coarse grain size. This allows detecting a misorientation distribution in a whole area of the grain. It can be seen that $\Delta\Theta$ in Fig. 4(a) does not exceed generally 2° except some spots with $\Delta\Theta \geq 3$–5°, which corresponds to subboundaries presented in initial structure (Fig. 3(a)). The first pass of ECAP introduces in turn many deformation-induced new boundaries with misorientations from 4 to 6° in grain center to 9 to 12° in the boundary regions (Fig. 4(b)). It should be noted that such boundaries located near mantle regions have generally a relatively large misorientation and their density increases rapidly by ECAP processing. This indicates that highly heterogeneous deformation takes place within initial grain interiors, leading to local lattice rotation and then formation of dislocation subboundaries. The latter may correspond to the boundaries of deformation bands and/or geometrically necessary boundaries (GNBs), which are able to be introduced into an Al alloy even under hot deformation conditions, as discussed in detail elsewhere [21,48]. Fig. 4(c) also shows the variation of $\Delta\Theta$ developed in a typical grain deformed to $\varepsilon = 2$. It can be seen that the $\Delta\Theta$ for some boundaries of deformation bands rises rapidly up to values of HABs, evolved after the second ECAP.

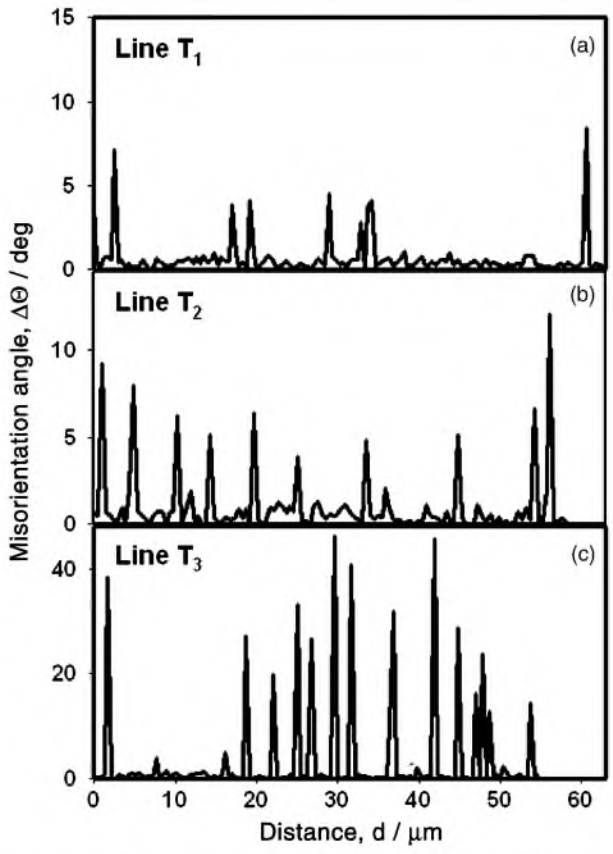

Fig. 4. Misorientation distribution of strain-induced (sub)grain and dislocation boundaries in Al–6% Mg–0.3% Sc alloy developed along the lines: (a) T_1, (b) T_2 and (c) T_3 indicated in Fig. 3. Note the different scale in (c).

3.4. TEM microstructures

Fig. 5 represents the typical TEM microstructures and the selected area electron diffraction (SAED) patterns for the samples (a) before ECAP and (b)–(d) pressed to various strains by ECAP at 450 °C. Objective apertures of 10 μm in diameter were employed for SAED analysis. It can be seen in Fig. 5(a) that the preliminary thermomechanical treatment (see Section 2) provides the formation of a well-developed subgrain structure composed of the equiaxed crystallites with an average size of around 1.6 μm. This microstructure is replaced by a new coarser subgrain structure after the first pass of hot ECAP (Fig. 5(b)). The TEM microstructures developed with further ECAP at low-to-moderate strains (Fig. 5(c)) comprise the crystallite aggregates with a preferred rectangular shape having low and medium angle misorientations (see the SAED pattern). The shape and size of the crystallites presented in Fig. 5(c) do not change significantly with strain up to 12 (Fig. 5(d)). However, the ring-like SAED pattern with scattered diffraction spots demonstrates the increased misorientation of such deformation-induced structures. This suggests that the microstructure composed of polycrystalline fine grains surrounded by HABs evolved continuously during ECAP through the fragmentation of crystallites by layered dislocation (sub)boundaries. It should also be noted that the evolution process of new grains can often be accompanied by a local grain boundary migration, as indicated by arrows in Fig. 5(d). It is known that the tetragonal shape of crystallites is unstable due to the presence of triple and quadruple junctions with angles close to 90° [43]. The limited grain boundary migration results in a structure with a more stable

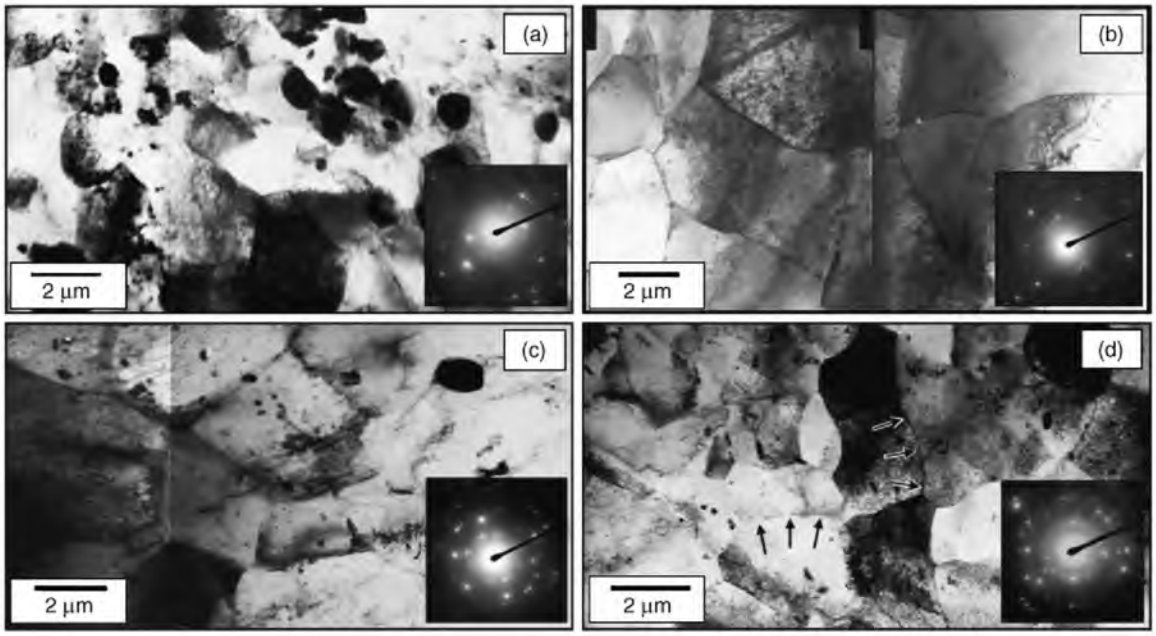

Fig. 5. Typical TEM microstructures and the diffraction patterns of Al–6% Mg–0.3% Sc alloy evolved during ECAP at 450 °C: (a) $\varepsilon = 0$, (b) $\varepsilon = 1$, (c) $\varepsilon = 4$ and (d) $\varepsilon = 12$.

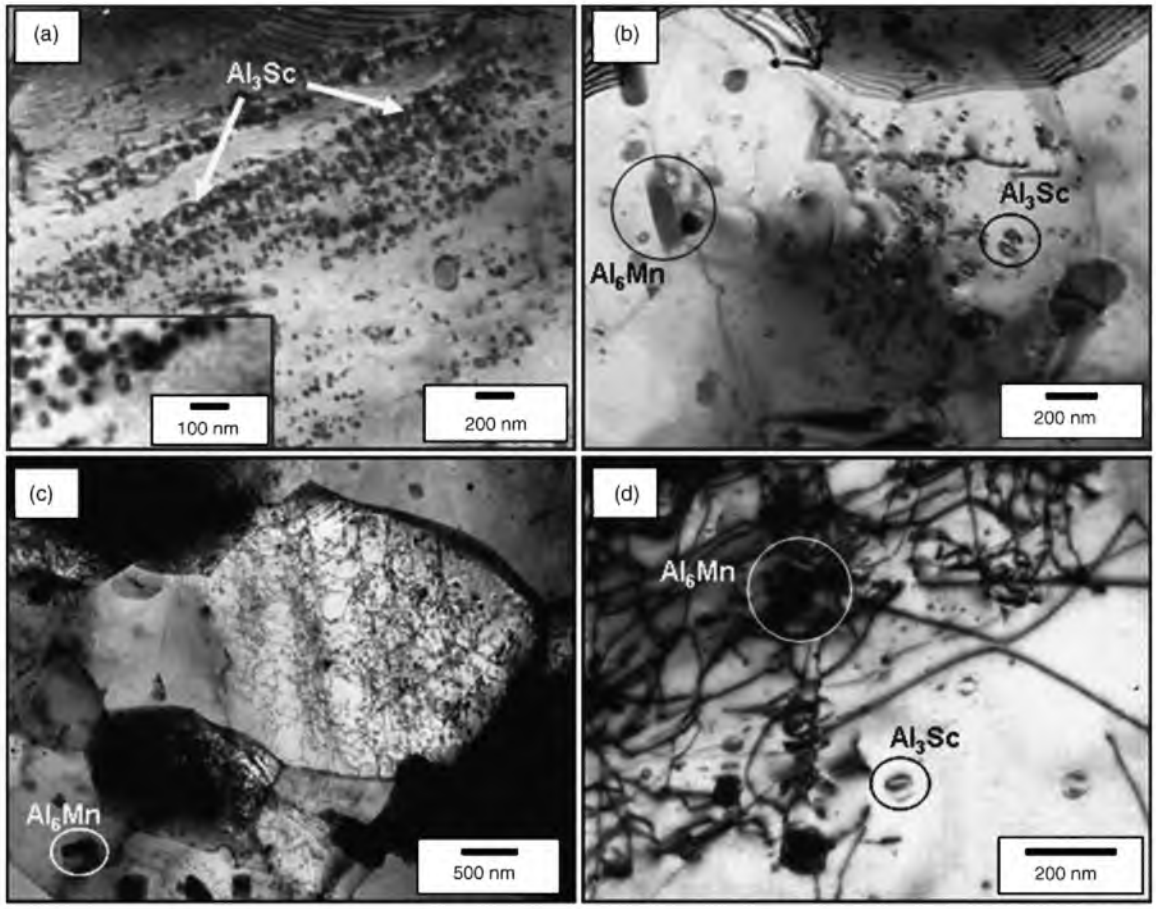

Fig. 6. Typical features of the secondary phase particles distribution in Al–6% Mg–0.3% Sc alloy at 450 °C: (a) $\varepsilon = 1$ and (b, c and d) $\varepsilon = 12$.

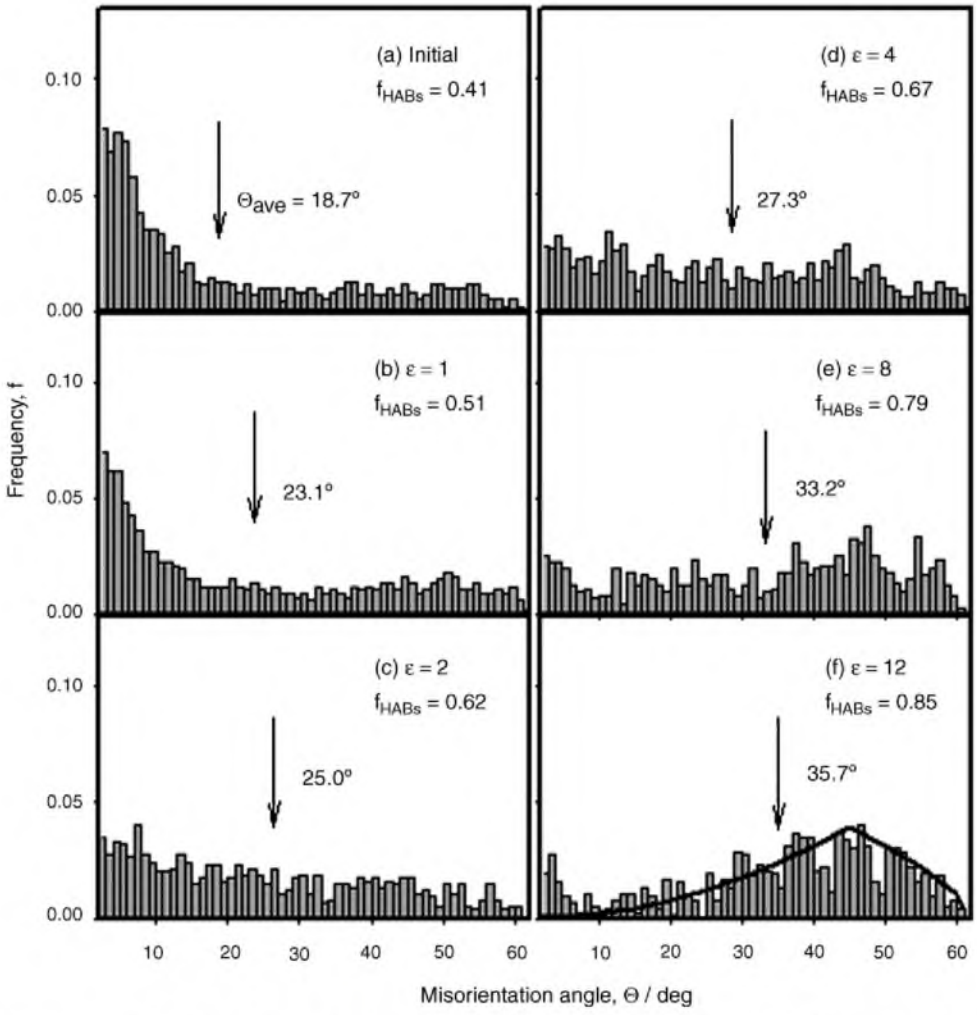

Fig. 7. Changes in misorientation distribution of dislocation and (sub)grain boundaries developed with straining by ECAP: (a) $\varepsilon = 0$, (b) $\varepsilon = 1$, (c) $\varepsilon = 2$, (d) $\varepsilon = 4$, (e) $\varepsilon = 8$ and (f) $\varepsilon = 12$. Θ_{ave} and f_{HABs} in (a)–(f) mean the average misorientation angle and fraction of high-angle boundaries, respectively. The solid line in (f) indicates the random misorientation distribution evaluated by Mackenzie [49].

configuration of boundaries and the triple junction angles close to 120°.[1]

Fig. 6 shows some typical features of the distribution of the secondary phase dispersion particles of Al_3Sc and Al_6Mn. These particles may be clearly recognized in TEM images due to a "coffee-bean" like contrast and a "pencil" like shape, respectively (e.g. [33]). It is seen in Fig. 6(a and b) that during hot ECAP of the present alloy, the particles may be distributed rather non-uniformly in grain interiors and form clusters and segregation bands. Fig. 6(c and d) demonstrate in turn the large numbers of dislocations that have strongly interacted with these Al_3Sc and Al_6Mn particles and distributed inhomogeneously even at a high strain of 12. It will be discussed in the *following sections* that such inhomogeneous distribution of lattice dislocations trapped by dispersoids can play a significant role in the development of heterogeneous dislocation substructures assisting further grain refinement.

3.5. Microstructure parameters

Fig. 7 represents changes in the misorientation distributions of deformation-induced dislocation boundaries derived from OIM analysis. It is seen in Fig. 7(a and b) that most of the boundaries developed before and after the first ECAP pass exhibit low-to-medium angle misorientations from 5 to 15°, as well as those above 15°, which were mainly developed by pre-treatment before ECAP. With further deformation, the fraction of low and moderate angle boundaries rapidly decreases and that of high-angle ones conversely increases in fine-grained regions (Fig. 7(c–f)); this is directly connected with the formation of new fine grains. Noteworthy that the average misorientation of 35.7° in Fig. 7(f) at $\varepsilon = 12$ is less than that of 40.7°, predicted by Mackenzie for randomly misoriented polycrystalline aggregates of cubic metals [49]. This difference may be attributed

[1] Note that in comparison with low-to-moderate angle boundaries, random HABs have a large potential to migrate due to their larger grain boundary energy [43]. This explains the fact that the formation of an equiaxed grain structure may be strongly followed by the transformation of LABs into HABs and so, becomes significant at relatively high strains.

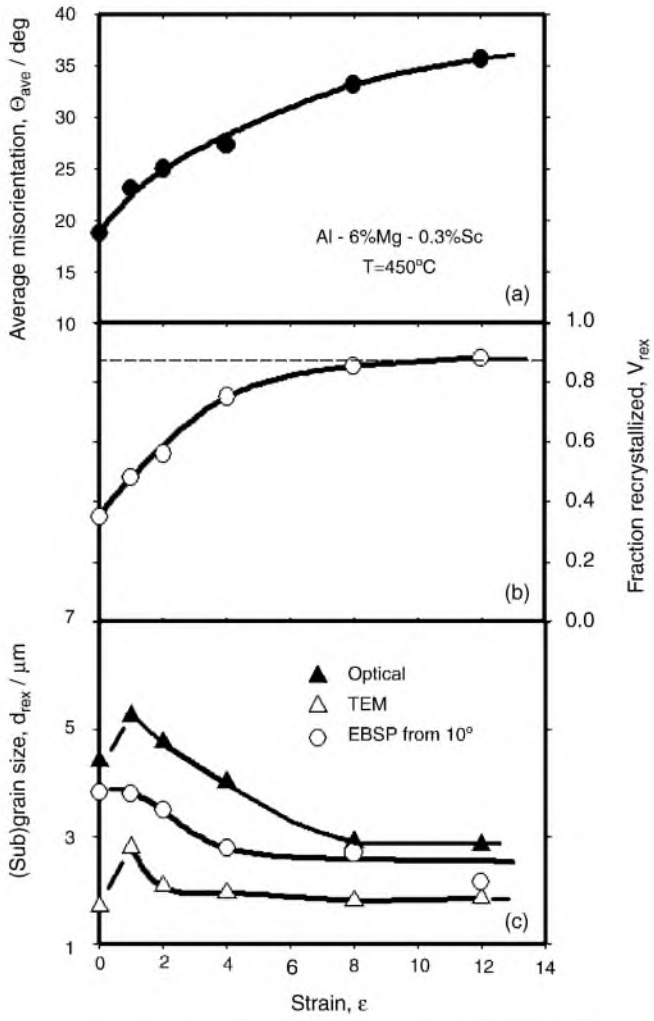

Fig. 8. Effect of hot ECAP on: (a) the average misorientation of dislocation/(sub)grain boundaries, Θ_{ave}, in the fine-grained regions; (b) the fraction of fine grains, V_{rex}; and (c) the average (sub)grain size evolved, d_{rex}.

to the strain-induced microstructure evolved through grain fragmentation, in which a fraction of low- and low-to-medium angle boundaries is always present.

Strain dependencies of (a) the average misorientation, Θ_{ave}, in the regions of newly developed grains; (b) their volume fraction, V_{rex}; and (c) the average (sub)grain size, d_{rex}, are depicted in Fig. 8. It can be seen in Fig. 8(a and b) that both Θ_{ave} and V_{rex} start to increase from 18.7° and 0.35, respectively, which correspond to the structure, developed before ECAP, and rise at almost constant rates against strain at $\varepsilon \sim 6$ and approach to around 35.7° and 0.85 at higher strains.

The main results represented in Fig. 8(c) can be summarized as follows. The grain sizes derived from optical microscopy and (sub)grain size measured by TEM increase after the first pass through the die from 4.4 to 5.5 μm and from 1.6 to 2.8 μm, respectively, while the size of the crystallites surrounded by moderate and high-angle boundaries measured by EBSP remains to be almost stable and equal to 3.4 μm after the first pressing. During further ECAP to large strains, the sizes of the crystallites revealed by EBSP and optical microscopy monotonically decrease with strain in the strain interval from 1 to 4 and from 1 to 8, respectively, followed by a saturation value of about 2.8 μm. On the other hand, the (sub)grain size revealed by TEM drops to about 2 μm upon the second pressing and, subsequently, is not significantly affected by ECAP. It is evident from Fig. 8(c) that the final grain size obtained after large strain is of the order of the crystallite size surrounded by LABs observed by TEM. Referring to almost the same (sub)grain size, as well as progressive increase in misorientation and volume fraction of new grains during deformation, such a process of microstructure evolution as shown in Fig. 8 can be considered as continuous dynamic recrystallization (cDRX) [43].

4. Discussion

4.1. The evolution process of new grains

The results described above show that new grains are mainly developed due to grain fragmentation process accompanied by frequent evolution of deformation-induced subboundaries with low-to-moderate angle misorientation, which can be recognized as the boundaries of deformation bands [14]. It was recently reported [11,13,14,17,21,28–30,34,36,37,42,44,48] that under severe deformation conditions at low to high temperatures, original grains can be subdivided by deformation bands, followed by evolution of fine crystallite components at high strains, and such a process can play an important role in grain refinement. During cold-to-warm IPS, the formation of deformation bands occurs because it is energetically easier for a grain to deform, if it is split into deformation bands, where the number of slip systems required for constrained deformation are fewer than 5 [29,45]. It has also been pointed out [21,30] that inhomogeneous deformation characteristics in ECAP itself can lead to the formation of deformation bands, which are developed by accommodation of strain gradients resulting from heterogeneous strains introduced by ECAP. Changes in shearing plane with repeated ECA pressings in route A can result in formation of deformation bands with different orientations [21]. A mechanism of grain refinement during IPS can be summarized as follows [21,30,44,48,50,51]. Repeated deformation results in an increase in the number and misorientation of the boundaries of deformation bands. Their mutual crossing leads to continuous fragmentation of coarse grains into misoriented domains. The boundary misorientations of these domains grow progressively with increasing strain, followed by their transformation into new grains surrounded by high-angle boundaries. It has been clearly shown [44] that such development of new fine grain structure is the consequence of kind of deformation-induced continuous reactions, i.e. cDRX.

The same discussion can be applied to the structural mechanism that operates during hot ECAP of the current alloy, in which the same sequence of structural changes leading to almost complete evolution of new fine grains can be clearly revealed (Figs. 2–8). It is noted, however, that heterogeneous deformation introduced by ECAP should normally decrease with increasing temperature [8,11,13,30]. Dislocation motion occurs more homogeneously at elevated temperatures and, even if any strain

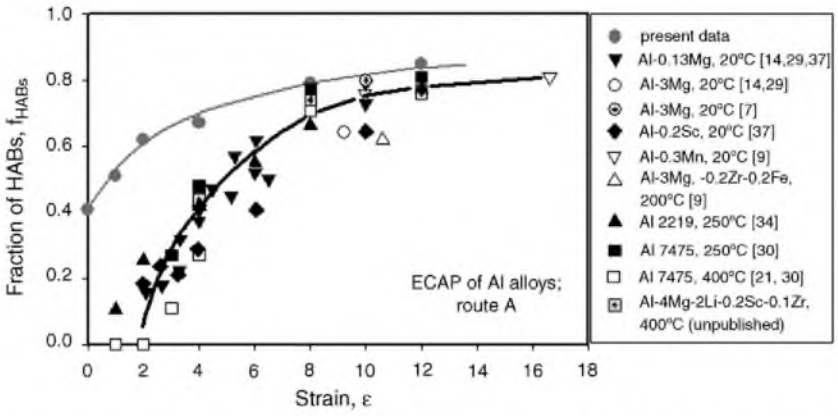

Fig. 9. Strain dependence of the fraction of HABs developed in Al–6% Mg–0.3% Sc alloy during ECAP at 450 °C and its relevance to reference data [7,9,14,21,22,29,30,34,37].

gradients are formed on a mesoscale due to a specific deformation mode introduced by ECAP, as mentioned above, they should rapidly disappear by frequent operation of some relaxation processes, including dynamic recovery and grain boundary sliding (GBS) [43,48]. As a result, deformation bands following high strain gradients could scarcely develop/rapidly relaxed under hot ECAP conditions of conventional Al alloys (e.g. [11,13]). In the present alloy with Sc and Mn additions, in contrast, the high fractions of nanoscale dispersoids of Al_6Mn and mostly Al_3Sc can serve as very effective stabilizers for dislocation substructures, as it was shown in Fig. 6, and thus retard or prevent any relaxation of strain gradients in grain interiors promoting the strain accumulation from pass to pass even during hot deformation. Moreover hot ECAP may provide inhomogeneous distribution of the particles within initial coarse grains (Fig. 6(a and b)). This additionally increases the strain inhomogeneity.

On the other hand, increasing deformation temperature may be very important for acceleration of dynamic recovery in the present alloy to provide grain refinement. It has been concluded [37] that strong inhibition of recovery and homogenization of slip may take place in dispersoid-containing alloys at low temperatures. This makes deformation bands more diffuse and so, represses their transformation into HABs. It is apparent that an elevated deformation temperature, in contrast, may promote the higher rate of dislocation rearrangement within the boundaries of deformation bands. This allows a greater possibility for them to become permanent boundaries, which then increase their misorientation with strain.

4.2. *Effect of initial structure on grain refinement*

The ECAP technique is considered presently as one of the most valuable scientific tools for studying the microstructure development in large strain deformation. As a rule, well-annealed and/or as-cast coarse-grained materials have been used as subjects in such laboratory investigations. Any effect of the initial microstructure of *pre-worked commercial alloys* on the microstructural development during ECAP is, however, not clear, to the best of the authors' knowledge. Fig. 9 summarizes the data reported in literature on strain dependence of the fractions of HABs developed in some Al alloys in route A under cold-to-hot ECAP conditions [7,9,14,21,22,29,30,34,37].[2] It can be seen in Fig. 9 that the fraction of HABs in the present pre-deformed alloy starts to rapidly increase just after first pass through the die and, in contrast, that in other Al alloys is retarded clearly up to $\varepsilon_c \geq 2$ [30]. This suggests that the present structure developed by the preliminary thermomechanical treatment is very much effective for the dynamic evolution of new fine grains. Note that the strain dependence of the fraction of HABs in the present alloy (Fig. 9) is correlated with that of V_{rex} and Θ_{ave} presented in Fig. 8. Namely, the rapid growth of HABs fraction at early stages of deformation can occur through the rapid generation/increase in misorientation of dislocation subboundaries in the initial structure; this corresponds to the rapid increase in V_{rex} and Θ_{ave}. Hence, there may be several factors accelerating grain refinement.

4.2.1. *Inhomogeneous grain structure*

It should be remembered in Figs. 2(a) and 3(a) that just before ECAP, the current alloy has a fraction of fine grains in the initial structure, which are inhomogeneously distributed along original grain boundaries. Under the present hot ECAP conditions (i.e. especially at $T = 450$ °C and $\varepsilon \approx 10^{\circ}\,s^{-1}$), this fine-grained structure can readily support GBS, as it was well documented for the same alloy in Ref. [35]. At the same time, GBS can hardly operate along the boundaries of coarse and elongated original grains. Plastic flow, therefore, should be mainly localized in the fine-grained mantle regions. As a result, additional high strain gradients can be injected in the columnar grains, followed by development of deformation bands even at early stages of hot deformation to collectively maintain their compatibility with surrounding fine grains. This can further enhance any heterogeneous strains introduced by ECAP. It is also interesting to note in

[2] The similar collected data, regarding the effect of strain on HABs fraction in aluminums, have been previously presented and discussed in detail elsewhere [22,30].

this context that in the present alloy, the newly evolved granular structure is developed heterogeneously during cDRX, making up the mantle of fine grains (Fig. 2). This is because the highest strain gradients can be introduced in the grain boundary- (and/or near-mantle-) regions compared to those in grain interiors [52]. Deformation bands with large misorientation are readily developed at the earlier stages of deformation in these regions (Fig. 4), leading to more rapid evolution of new grains.[3]

4.2.2. *Well-developed substructures*

From Fig. 5, it is evident that initial subgrain structure introduced by the preliminary thermomechanical treatment is completely rearranged after the first pressing and a new dynamically equilibrium state with larger subgrain size is evolved at hot ECAP. Accordingly, it cannot play any remarkable role in new fine grain evolution during ECAP. This is in consistent with a conclusion that new HABs are not formed via a gradual increase in misorientation of low-angle subgrain boundaries [37,51]. In contrast, the low-to-medium angled boundaries with misorientation 5–15° presented in the initial microstructure can be involved in the process of grain refinement (Fig. 4). These boundaries may be resulted from deformation bands developed by prior extrusion and exist stably during high-temperature exposure just before hot deformation. They can be frequently intersected with deformation bands produced at the earlier stages of ECAP. This results in the rapid evolution of new equiaxed crystallites with a stable grain size and therefore significantly accelerates kinetics of grain refinement [50].

On the other hand, it is seen in Fig. 9 that irrespective of initial structure, the kinetics of grain refinement is retarded, when the fraction of HABs is around 0.6–0.7 and, with further processing, the population of HABs approaches the similar saturation values of around 0.8 with some scatter. In the present alloy, the HABs fraction, $f_{HABs} = 0.6–0.7$, is achieved at a strain of around 4 (Fig. 9), at which, as it is seen in Fig. 8, both V_{rex} and the size of crystallites surrounded by moderate-to-high angle boundaries start to saturate. This suggests that the development of new deformation bands tends to be expired at this strain and subsequent increase in HABs may be mainly accompanied by gradual increase in the misorientation, Θ_{ave}, of subboundaries introduced into the microstructure at the earlier stages of deformation. This inhibition of grain refinement may be because any strain gradients required for newly generated deformation bands can be relaxed in fine-grained regions, which are continuously developed during deformation [48,50].

4.3. *Influence of ECAP regimes on newly generated grain size*

The results from present experiments, as documented in Fig. 8, reveal that an equilibrium grain size of around 2.8 μm can be introduced at high strains into the Al–Mg–Sc alloy during ECAP at 450 °C and at $3\,s^{-1}$. To evaluate the effect of deformation conditions and alloy chemical composition on the grain refinement in the present alloy, the grain size obtained has been compared to the structures developed in other Al alloys processed under various ECAP conditions.

It is known [43,54,55] that the effect of the deformation variables such as strain rate and deformation temperature on the microstructure developed in various deformation schemes can be represented using Zener-Hollomon parameter (Z):

$$Z = \dot{\varepsilon} \exp\left(\frac{Q}{RT}\right), \tag{1}$$

where Q is the activation energy for plastic deformation and R (=8.31 J/mol K) is the universal gas constant and other have the usual meanings. Fig. 10 represents the relationship between Z parameter and the size of newly generated (sub)grains in a variety of Al alloys processed to large strains by ECAP, for which a full body of experimental results, allowing evaluation of the effective strain rate and equilibrium (sub)grain size, is available in literature [5,6,8,11–13,15,17–19,23–28,30–35,38,40–42]. Besides, the results reviewed in Fig. 10 are also partially based on some our own unpublished data. The strain rate during ECAP was estimated using analytical equations and graph presented in Ref. [47]. The activation energy of self-diffusion in Al, which is 142 kJ/mol [56], was taken into account for estimating Z parameter.

It is seen in Fig. 10 that at $Z \leq 10^{15}\,s^{-1}$, the minimum (sub)grain size that can be achieved by ECAP in Al alloys decreases with increasing Z to obey the linear relationship in the double logarithm scale as

$$d_{rex} \sim Z^{-0.22}. \tag{2}$$

The fact that Z parameter determines the grain size reveals that development of fine grain structures during ECAP is closely related to thermal activation processes [43,55]. As it is generally considered that the microstructural evolution in Al alloys occurs mainly through dynamic recovery, which enhances the rearrangement of the dislocation substructures during deformation and assists the formation of new equiaxed (sub)grains [43], it is evident that the smaller (sub)grain size can be obtained through decreasing rate of dynamic recovery. The (sub)grain size is also finer in alloys that contain elements that have a strong effect on inhibiting recovery, such as Mg, Sc, Li, Zr, etc. [5,31,37]. Note here that the grain size achieved during hot ECAP in the present Al–Mg–Sc alloy can be in a good agreement with those in such heavily alloyed materials developed under appropriate Z conditions.

It can be also seen in Fig. 10 that at $Z > 10^{15}\,s^{-1}$, the dependence of grain size on Z parameter becomes much weaker irrespective of alloy's chemical composition, so that variations in temperature and/or strain rate can produce relatively small changes in grain size.[4] The present consideration suggests that

[3] Such structural behavior of cDRX looks similar to that of the "necklace" dynamic recrystallization, which takes place in low stacking fault energy materials during hot working [53] although their physical mechanisms are completely different.

[4] It should be noted that the elementary deformation mechanisms are apparently changed in Al alloys at lower temperatures or/and large strain rates and

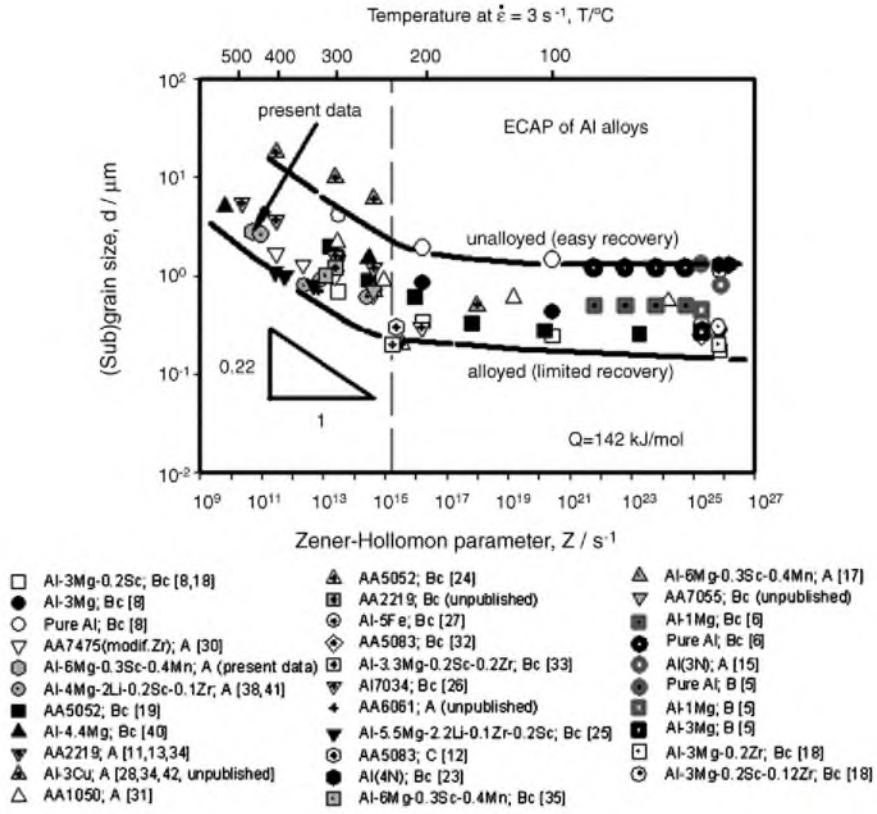

Fig. 10. Relationship between Z parameter and equilibrium (sub)grain size evolved during ECAP in various Al alloys [5,6,8,11–13,15,17–19,23–28,30–35,38,40–42]. The upper scale indicates the temperature corresponding to the present ECAP conditions.

any effort to severely refine the grain structure by decreasing ECAP temperature and/or increasing pressing speed under high Z conditions may be almost unavailing and so, a processing window to obtain (ultra)fine grain structure in a majority of low-alloyed Al alloys is relatively small. On the contrary, as it has been demonstrated in the present work, a fairly fine grain structure may be introduced into a heavily alloyed and/or hard-to-deform Al alloy even at ECAP temperature as high as $0.8T_m$. This implies that there is a big potential for obtaining very fine grain size in these alloys at elevated temperatures alleviating the difficulties of ECAP.

5. Summary

Microstructural evolution in a commercial Al–6% Mg–0.4% Mn–0.3% Sc alloy subjected to ECAP at $T=450\,^{\circ}C$ (around $0.8T_m$) was examined in the present work. The alloy was pre-strained by extrusion at 390 °C to a strain of about 0.7, followed by annealing at 400 °C for 1 h before ECAP. The main results can be summarized as follows:

(1) ECAP results in a considerable grain refinement. A new fine-grained microstructure with an average crystallite size of about 2.8 μm develops at large strains above 8. The new grains are evolved first in the mantle regions and propagated into the original grain interiors with further straining.

(2) Prior warm extrusion and annealing develop a fragmented coarse-grained structure with a remarkable fraction of fine grains in the mantle regions. Such initial microstructure accelerates dynamic evolution of high-angle boundaries during subsequent hot ECAP and is an important prerequisite for grain refinement.

(3) Inhomogeneous deformation occurring during hot ECAP leads to formation of deformation bands. Repeated ECAP results in mutual crossing, increase in number and misorientation of deformation bands followed by transformation of the boundaries of deformation bands into high-angle ones and evolution of new fine grains at high strains. It is concluded that such grain refinement process occurs in accordance with a deformation-induced continuous reaction; that is essentially similar to cDRX.

(4) The high fractions of nanoscale dispersoid phase Al_6Mn and mostly coherent Al_3Sc formed in the present alloy are very effective in dislocation pinning and so may retard or prevent any relaxation of large strain gradients that are required for development of deformation bands. The pres-

cannot be controlled by self-diffusion (e.g. [56]). In this case, the dependence of grain size on Z calculated through the activation energy for self-diffusion does not have any physical meaning. Z may be considered only as a technological parameter combining effects of temperature and strain rate on the deformation microstructure.

ence of transition metal alloying elements such as Sc and Mn can be considered, therefore, to be an important factor promoting the evolution of deformation bands and subsequent grain refinement under high temperature ECAP conditions. This can be further enhanced by inhomogeneous distribution of the particles in grain interiors during hot ECAP.

(5) The equilibrium (sub)grain size developed during ECAP of Al alloys can be generally defined by temperature, strain rate (combined by Zener-Hollomon parameter, Z) and chemical composition of the alloy. The grain size achieved in the present alloy is in a good agreement with those in other heavily alloyed Al alloys developed under appropriate Z conditions.

Acknowledgements

One of the authors (O.S.) would like to express his thanks to the National Institute for Materials Science for providing a scientific fellowship. The authors acknowledge with gratitude the financial support received from the Light Metals Educational Foundation of Japan and Deutsche Forschung Gemeinschaft (DFG) under Grant No. 01-02-04004. The authors also wish to acknowledge Miss R. Babicheva for help in experimental work.

References

[1] R.Z. Valiev, R.K. Islamgaliev, I.V. Alexandrov, Prog. Mater. Sci. 45 (2000) 103–189.
[2] V.M. Segal, Mater. Sci. Eng. A197 (1995) 157–164.
[3] Y. Iwahashi, Z. Horita, M. Nemoto, T.G. Langdon, Acta Mater. 45 (1997) 4733–4741.
[4] C. Harris, S.M. Roberts, P.B. Prangnell, F.J. Humphreys, in: T. McNelley (Ed.), Proceedings of ReX'96: The Third International Conference on Recrystallization and Related Phenomena, Monterey Institute of Advanced Studies, Monterey, CA, 1997, pp. 587–594.
[5] Y. Iwahashi, Z. Horita, M. Nemoto, T.G. Langdon, Metall. Mater. Trans. A29 (1998) 2503–2510.
[6] P.B. Berbon, M. Furukawa, Z. Horita, M. Nemoto, T.G. Langdon, Metall. Mater. Trans. A30 (1999) 1989–1997.
[7] J.S. Hayes, R. Keyte, P.B. Prangnell, Mater. Sci. Technol. 16 (2000) 1259–1263.
[8] A. Yamashita, D. Yamaguchi, Z. Horita, T.G. Langdon, Mater. Sci. Eng. A287 (2000) 100–106.
[9] A. Gholinia, P.B. Prangnell, M.V. Markushev, Acta Mater. 48 (2000) 1115–1130.
[10] J.R. Bowen, P.B. Prangnell, F.J. Humphreys, Mater. Sci. Technol. 16 (2000) 1246–1250.
[11] O.S. Sitdikov, R.O. Kaybyshev, I.M. Safarov, I.A. Mazurina, Phys. Met. Metallogr. 92 (2001) 270–280.
[12] S.Y. Chang, J.G. Lee, K.T. Park, D.H. Shin, Mater. Trans. 42 (2001) 1074–1080.
[13] R. Kaibyshev, O. Sitdikov, I. Mazurina, D. Lesuer, in: T. Chandra, K. Higashi, C. Suryanarayama, C. Tome (Eds.), Proceedings of Thermec'2000 International Conference, J. Mater. Process. Technol.-CD Version, 2001 (Special issue).
[14] P.B. Prangnell, J.R. Bowen, A. Gholinia, in: A.R. Dinesen, M. Eldrup, D. Juul Jensen, S. Linderoth, T.B. Pedersen, N.H. Pryds, A. Schroder Pedersen, J.A. Wert (Eds.), Science of Metastable and Nanocrystalline Alloys, Structure Properties and Modelling, Proceedings of the 22nd Riso International Symposium on Materials Science, Riso National Laboratory, Roskilde, 2001, pp. 105–126.
[15] J.Y. Chang, J.S. Yoon, G.H. Kim, Scripta Mater. 45 (2001) 347–354.
[16] S.D. Terhune, D.L. Swisher, K. Oh-Ishi, Z. Horita, T.G. Langdon, T.R. McNelley, Metall. Mater. Trans. A33 (2002) 2173–2184.
[17] R. Kaibyshev, O. Sitdikov, S. Olenyov, in: Y.T. Zhu, T.G. Langdon, R.S. Mishra, S.L. Semiatin, M.J. Sharan, T.C. Lowe (Eds.), Ultrafine Grained Materials II, TMS, San Diego, 2002, pp. 65–74.
[18] S. Lee, A. Utsunomiya, H. Akamatsu, K. Neishi, M. Furukawa, Z. Horita, T.G. Langdon, Acta Mater. 50 (2002) 553–564.
[19] Y.C. Chen, Y.Y. Huang, C.P. Chang, P.W. Kao, Acta Mater. 51 (2003) 2005–2015.
[20] A. Vinogradov, A. Washikita, K. Kitagawa, V.I. Kopylov, Mater. Sci. Eng. A349 (2003) 318–326.
[21] A. Goloborodko, O. Sitdikov, T. Sakai, R. Kaibyshev, H. Miura, Mater. Trans. 44 (2003) 766–774.
[22] O.V. Mishin, D. Juul Jensen, N. Hansen, Mater. Sci. Eng. A342 (2003) 320–328.
[23] C. Xu, T.G. Langdon, Scripta Mater. 48 (2003) 1–4.
[24] T.L. Tsai, P.L. Sun, P.W. Kao, C.P. Chang, Mater. Sci. Eng. A342 (2003) 144–151.
[25] R.K. Islamgaliev, N.F. Yunusova, R.Z. Valiev, N.K. Tsenev, V.N. Perevezentsev, T.G. Langdon, Scripta Mater. 49 (2003) 467–472.
[26] C. Xu, M. Furukawa, Z. Horita, T.G. Langdon, Acta Mater. 51 (2003) 6139–6149.
[27] V.V. Stolyarov, R. Lapovok, I.G. Brodova, P.F. Thomson, Mater. Sci. Eng. A357 (2003) 159–167.
[28] R. Kaibyshev, I. Mazurina, I. Denisova, O. Sitdikov, in: Z. Jin, A. Beaudoin, T.A. Bieler, B. Radhakrishnan (Eds.), Hot Deformation of Aluminum Alloys III, TMS, Seattle, 2003, pp. 151–157.
[29] P.B. Prangnell, J.R. Bowen, P.J. Apps, Mater. Sci. Eng. A375–377 (2004) 178–185.
[30] A. Goloborodko, O. Sitdikov, R. Kaibyshev, H. Miura, T. Sakai, Mater. Sci. Eng. A381 (2004) 121–128.
[31] Y.Y. Wang, P.L. Sun, P.W. Kao, C.P. Chang, Scripta Mater. 50 (2004) 613–617.
[32] V.V. Stolyarov, R. Lapovok, J. Alloys Compd. 378 (2004) 233–236.
[33] H.B. Geng, S.B. Kang, B.K. Min, Mater. Sci. Eng. A373 (2004) 229–238.
[34] R. Kaibyshev, I. Mazurina, Mater. Sci. Forum 467–470 (2004) 1251–1260.
[35] F. Musin, R. Kaibyshev, Y. Motohashi, G. Itoh, Metall. Mater. Trans. A35 (2004) 2383–2392.
[36] K. Furuno, H. Akamatsu, K. Oh-ishi, M. Furukawa, Z. Horita, T.G. Langdon, Acta Mater. 52 (2004) 2497–2507.
[37] P.J. Apps, M. Berta, P.B. Prangnell, Acta Mater. 53 (2005) 449–511.
[38] R. Kaibyshev, K. Shipilova, F. Musin, Y. Motohashi, Mater. Sci. Eng. A396 (2005) 341–351.
[39] I. Gutierrez-Urrutia, M.A. Munoz-Morris, D.G. Morris, Mater. Sci. Eng. A394 (2005) 399–410.
[40] M. Popovic, B. Verlinden, Mater. Sci. Technol. 21 (2005) 606–612.
[41] R. Kaibyshev, K. Shipilova, F. Musin, Y. Motohashi, Mater. Sci. Technol. 21 (2005) 408–418.
[42] I. Mazurina, A. Goloborodko, R. Kaibyshev, H. Miura, T. Sakai, Mater. Sci. Forum 503–504 (2006) 829–834.
[43] F.J. Humphreys, M. Hatherly, Recrystallization and Related Annealing Phenomena, Pergamon Press, Oxford, 1996.
[44] A. Belyakov, T. Sakai, H. Miura, K. Tsuzaki, Philos. Mag. A81 (2001) 2629–2643.
[45] B. Bay, N. Hansen, D.A. Hughes, D. Kuhlmann-Wilsdorf, Acta Metall. Mater. 40 (1992) 205–219.
[46] Y.A. Filatov, V.I. Yelagin, V.V. Zacharov, Mater. Sci. Eng. A280 (2000) 97–101.
[47] H.S. Kim, J. Mater. Res. 17 (2002) 172–179.
[48] O. Sitdikov, T. Sakai, A. Goloborodko, H. Miura, R. Kaibyshev, Philos. Mag. 85 (2005) 1159–1175.
[49] J.K. Mackenzie, Biometrika 45 (1958) 229–240.

[50] O. Sitdikov, T. Sakai, A. Goloborodko, H. Miura, R. Kaibyshev, Mater. Trans. 45 (2004) 2232–2238.
[51] O.S. Sitdikov, A.N. Goloborod'ko, R.O. Kaibyshev, H. Miura, T. Sakai, Phys. Met. Metallogr. 99 (2005) 106–117.
[52] A. Belyakov, W. Gao, H. Miura, T. Sakai, Metall. Mater. Trans. A29 (1998) 2957–2965.
[53] T. Sakai, J.J. Jonas, Acta Metall. 32 (1984) 189–209.
[54] S.L. Semiatin, P.B. Berbon, T.G. Langdon, Scripta Mater. 44 (2001) 135–140.
[55] A. Ohmori, S. Torizuka, K. Nagai, N. Koseki, Y. Kogo, Mater. Trans. 45 (2004) 2224–2231.
[56] H.J. Frost, M.F. Ashby, Deformation-Mechanism Maps: The Plasticity and Creep of Metals and Ceramics, Pergamon Press, Oxford, New York, 1982.